Journal of
Molluscan Studies

The Malacological Society of London

Journal of Molluscan Studies (2015) **81**: 442–454. doi:10.1093/mollus/eyv021
Advance Access publication date: 14 June 2015

The Miocene genus *Mantellina* (Bivalvia: Limidae) discovered living on the deep reefs off Curaçao, with the description of a new species

M. G. Harasewych[1] and I. Tëmkin[1,2]

[1]*Department of Invertebrate Zoology, MRC-163, National Museum of Natural History Smithsonian Institution, PO Box 37012, Washington, DC 20013-7012, USA; and* [2]*Department of Biology, Northern Virginia Community College, 4001 Wakefield Chapel Road, Annandale, VA 22003-3796, USA*

Correspondence: M.G. Harasewych; e-mail: harasewych@si.edu

(Received 3 December 2014; accepted 6 April 2015)

ABSTRACT

Mantellina translucens n. sp. inhabits the deep reefs (215–310 m) off southeastern Curaçao, occurring singly or in pairs, attached to vertical rock walls and boulders by thin byssal threads. This species differs from all living Limidae in having an exceptionally thin, comarginally corrugated shell that is longer than tall and lacks radial sculpture. This new species possesses a unique suite of characters associated with adaptations to an epibyssate mode of life in bathyal habitats, including simplification of the digestive tract, possibly indicating omnivory. It is assigned to the genus *Mantellina* Sacco, 1904, previously known only from fossil deposits of Burdigalian to Serravallian Miocene age of the Central Paratethys, on the basis of similar shell morphology. Anatomical characters and ribosomal DNA sequence data (18S and 16S genes) confirm placement of this taxon within the family Limidae, yet its shell superficially resembles those of several genera of the extinct family Inoceramidae, while differing in hinge morphology and shell ultrastructure. A preliminary molecular phylogeny recovered Limidae as a monophyletic clade within Pteriomorphia, with *Mantellina* derived relative to *Limaria*, and sister group to a clade containing the remaining representatives of Limidae. *Ctenoides* was not monophyletic. The phylogenetic tree based on molecular data does not support previously proposed suprageneric relationships based on morphological data.

INTRODUCTION

With origins in the Carboniferous (Mississippian) and an extensive fossil record, the family Limidae is represented in the Recent fauna by eight genera and over 130 species that occur in all oceans, ranging from tropical to polar regions and from subtidal to abyssal depths (Huber, 2010; Coan & Valentich-Scott, 2012; Gofas, 2014). Thirty-nine species, representing nine genera, have so far been reported from the western Atlantic Ocean (Rosenberg, 2009). Recent investigations of deep-reef communities off southeastern Curaçao, using the research submersible *Curasub*, have encountered an uncommon but conspicuous limid that lives bysally-attached to vertical rock faces at bathyal depths. This large, distinctive and fragile species is not referable to any presently known Recent genus of Limidae. A review of the fossil literature revealed close morphological similarities to the genus *Mantellina* Sacco, 1904, described on the basis of a single, partial specimen from Miocene deposits in the hills surrounding Turin, Italy. The shell morphology, anatomy and ecology of this new species are described, and its relationships to other living limids inferred based on 18S rDNA and 16S rDNA sequence data.

MATERIAL AND METHODS

Specimens and morphological observations

Specimens were photographed *in situ* and collected using the research submersible *Curasub* at several locations off the Sea Aquarium in Willemstad, Curaçao, and preserved directly in 95 % ethanol. Fine details of the shell and its microstructure were examined on shells and fragments that were cleaned with bleach (NaClO), rinsed in distilled water, immersed in liquid nitrogen to increase brittleness prior to fracturing, then coated with gold and photographed using a Leica Stereoscan 440 scanning electron microscope. Three paratypes were dissected using standard techniques (see Bieler *et al.*, 2014), including the use of aqueous toluidine blue to enhance visibility of internal structures.

Type specimens were deposited in National Museum of Natural History, Smithsonian Institution, Washington D.C. (USNM), Natural History Museum, London (NHMUK) and Netherlands Centre for Biodiversity Naturalis, Leiden (NNML).

Molecular studies

Genomic DNA was extracted from portions of the mantle edge (*c.* 25 mg) of the holotype using the DNeasy Tissue Kit (Qiagen) according to the manufacturer's animal tissue protocol. The 16Sar and 16Sbr primers (Palumbi, 1996) were used to amplify a section of the 16S rDNA gene. The partial 18S gene was amplified using the Euk-A/Euk-B primer set (Medlin *et al.*, 1988) and single-stranded sequencing reactions were carried out with these primers and the internal forward and reverse primers of Harasewych *et al.* (1997). For each gene, the Promega GoTaq hot start master mix (Promega M7132) was utilized at concentrations according to the manufacturer's instructions, but modified to reduce the reaction volume to 20 μl. Cycling parameters for each gene region were optimized as follows: for 16S, initial denaturation for 7 min at 95 °C + 35 cycles (30 s at 95 °C + 45 s at 48 °C + 1 min at 72 °C) + 5 min at 72 °C; for 18S, initial denaturation for 7 min at 95 °C + 35 cycles (30 s at 95 °C + 45 s at 50 °C + 1 min at 72 °C) + 7 min at 72 °C. Polymerase chain reaction (PCR) products were visualized by agarose gel electrophoresis (1.5 % agarose) and purified with ExoSAP-IT (Affymetrix) according to the manufacturer's protocols prior to sequencing.

Sequencing reactions were performed using 1 μl of purified PCR product in a 10 μl reaction containing 0.5 μl primer, 1.75 μl Big Dye buffer and 0.5 μl Big Dye (Life Technologies). The sequencing reaction was carried out under standard cycling conditions (30 cycles of 30 s at 95 °C + 30 s at 50 °C + 4 min at 60 °C). Reactions were purified using Millipore Sephadex plates (MAHVN-4550) according to the manufacturer's instructions and sequenced on an ABI 3730XL automated DNA sequencer. Sequencher v. 4.7 (GeneCodes, Ann Arbor, MI, USA) was used to visualize, trim, edit and assemble contigs from forward and reverse sequences. The sequences have been deposited in GenBank (NCBI). Accession numbers are listed in Table 1.

Phylogenetic analyses

Sequences for the nuclear 18S rDNA and mitochondrial 16S rDNA genes were aligned against corresponding genes from representative species of seven (of nine) living limid genera, as well as a selection of outgroup taxa representing the remaining orders within Pteriomorphia (see Bieler *et al.*, 2014) that contain living species (Table 1).

Table 1. List of taxa and their GenBank Reference numbers for gene sequences used in phylogenetic analyses.

TAXON	18S rDNA	16S rDNA
Mytilus edulis	L33448.1	AY484747.1
Crassostrea virginica	KC429335.1	AY905542.2
Atrina rigida	KJ365956.1	KJ365702.1
Arcopsis adamsi	KC429327.1*	KC429245.1*
Barbatia barbata	KC429326.1*	KC429244.1*
Glycymeris glycymeris	KC429328.1*	KC429246.1*
Pecten maximus	L49053.1	KC429258.1
Propeamussium watsoni	KC429340.1*	KC429259.1*
Acesta excavata	GQ240893.1	AM494898.1*
Lima lima	KC429339.1*	KC429257.1*
Ctenoides annulata	AJ389653.1	EU379439.1
Ctenoides scaber	KC429338.1*	KC429256.1*
Limaria hians	AF120534.1	JQ611445.1
Limatula simillima	AJ422063.1*	AJ422064.1*
Antarctolima hodgsoni	AJ422062.1*	AJ422065.1*
Antarctolima ovalis	AJ422060.1	AJ422068.1
Antarctolima pygmaea	AJ422061.1	AJ422066.1
Mantellina translucens holotype	KP843862*	KP843861*

Asterisk denotes that the same animal was the source for sequences within the same species.

To circumvent alignment ambiguity in the analysis of the ribosomal DNA sequences, all potential nucleotide homologies were evaluated in the framework of dynamic homology (Wheeler, 2001), as implemented in POY v. 5.1.1 (Varón *et al.*, 2013). Initially, multiple alignments were constructed for each locus using MAFFT 7 (Katoh & Standley, 2013) under default parameters and partitioned into a total of 31 fragments flanked by highly conservative regions (lacking indels), with the gaps subsequently removed. Fragmenting DNA sequences allowed for reduction of computation time and ensured that the assignment of indels was restricted to unambiguously homologous regions. None of the regions were excluded from the analyses. The homology scheme corresponding to the topology of the optimal cladogram was used to produce an implied alignment (total length = 3,120 bp) (Wheeler, 2003a; Giribet, 2005), which was used for maximum likelihood (ML) analysis.

Phylogenetic analyses of DNA sequence data were performed under the parsimony optimality criterion using direct optimization (Wheeler, 1996) and under the ML optimality criterion using a static alignment. The latter were based on the implied alignment corresponding to the single optimal cladogram obtained from the parsimony analysis of the combined data performed by direct optimization under the equal-cost regime.

Parsimony analyses under direct optimization were executed in POY v. 5.1.1. Initially, 300 Wagner trees were generated by random-addition sequence and submitted to alternating subtree pruning and regrafting (SPR) and tree bisection and reconnection (TBR) branch swapping to completion. The optimal cladograms were subjected to 50 iterations of parsimony ratchet, upweighting 20 % of nucleotide characters by a factor of 5 and retaining one optimal cladogram per iteration. The resulting optimal cladograms were rediagnosed under iterative-pass optimization (Wheeler, 2003b). Parsimony analyses were conducted under equal costs regime and a weighting scheme that maximizes homology of both sequence fragments and individual nucleotide positions in the analysis of sequences of variable length (De Laet, 2005).

Given the optimal cladogram and the corresponding implied alignment concatenated for both loci, the best-fit model of substitution, estimated by jModelTest v. 2.1.7 (Darriba *et al.*, 2012) using the Akaike Information Criterion (AIC), corresponded to the transversion model that included estimation of the proportion of invariant sites and assumed a gamma distributed rate variation among sites (TVM + I + Γ; AIC = 26694.124). This substitution model was used for the ML analyses, as implemented in PhyML v. 3.0 (Guindon *et al.*, 2010), for 250 independent replicates using alternating nearest-neighbour interchange and SPR branch swapping.

The ensemble consistency index and the ensemble retention index for the optimal tree(s) were calculated in POY v. 5.1.1, with the dynamic-homology characters transformed into static nucleotide-level characters by static approximation (Wheeler, 2003a). The robustness of phylogenetic relationships was evaluated using jackknife support methods at nucleotide level. For calculating jackknife support values, 2,000 resampling iterations with 36 % of sites removed during each pseudoreplicate were performed using POY v. 5.1.1.

SYSTEMATIC DESCRIPTIONS

Subclass AUTOBRANCHIAGrobben, 1894
Superorder PTERIOMORPHIA Beurlen, 1944
Order LIMIDA Moore, 1952
Superfamily LIMOIDEA Rafinesque, 1815
Family LIMIDAE Rafinesque, 1815

Mantellina Sacco, 1904

Mantellum (*Mantellina*) Sacco, 1904: 148 (type species, *Mantellum inoceramoides* Sacco, 1904, by original designation).
Lima (Mantellina)—Cossmann, 1905: 90.
Mantellina—Vokes, 1967: 191.
Limaria (*Mantellina*)—Cox & Hertlein, 1969: N389; Schultz, 2001: 301.

Original description: "Shell small, thin, obliquely ovate; surface with concentric, undulating ribs, inoceramid-like" (Saccho, 1904: 148; translated from Latin). 'Inoceramid' refers to its resemblance to the family Inoceramidae Giebel, 1852, an extinct family of Pteriomorphia that ranged from the Late Permian to the Upper Cretaceous.

Diagnosis: Shell ovate, elongated (to 41 mm), very thin, delicate, weakly biauriculate, with anterior and posterior gapes. Surface broadly crenulated comarginally, lacking radial sculpture. Umbone orthogyrate, cardinal area broadly triangular, ligament alivincular, amphidetic.

Remarks: Mantellina was originally proposed as a subgenus of *Mantellum*. The genus *Mantellum* Röding, 1798 is an objective synonym of *Lima* Bruguière, 1797, as both have the same type species. Subsequent authors used this generic name in a different sense and *Mantellum* Mörch, 1853 (non Röding, 1798) has been synonymized with *Limaria* Link, 1807 (Cox & Hertlein, 1969: N389; Coan & Valentich-Scott, 2012: 321).

Sacco (1904) based this subgenus on a single, small, incomplete specimen of the type species, *Mantellina inoceramoides*, from fossil deposits (Serravallian Miocene) in the Turin Hills. He noted the resemblance of this genus and its type species to some members of the family Inoceramidae, with which it shares a thin shell with distinctive, broadly undulating comarginal sculpture. However, *Mantellina* lacks the multiple ligamental pits that are diagnostic of Inoceramidae and has an anterior gape, which is lacking in inoceramids. The morphology of the cardinal area and ligament indicate a relationship with the family Limidae, which is confirmed by anatomical features such as the foot being rotated 180° relative to its long axis, a feature unique to limoids (Bieler *et al.*, 2014) as well as by phylogenetic analyses based on partial sequences of both nuclear (18S) and mitochondrial (16S) genes.

Mantellina translucens n. sp.

(Figs 1–5)

Type material: Holotype (USNM 1265094), off Sea Aquarium, Bapor Kibra, Willemstad, Curaçao, 12° 04.90′N, 63° 53.74′W, on vertical wall of rock ridge at 279 m, coll. M. G. Harasewych, *Curasub* 13–06, 23 May 2013; paratypes 1–9 (USNM 1265095–1265098, 1265100, 1265102, 1265104–1265106), same loc., 279 m, M. G. Harasewych, coll., *Curasub* 13-06, 23 May 2013; paratypes 10–14 (USNM 1265107), paratype 15 (NHMUK 20150038), same loc., 275–305 m, coll. A. Schrier, *Curasub* 14–18, 24 September 2014; paratypes 16–20 (USNM 1265108), paratype 21 (NHMUK 20150039), same loc., 266–302 m, coll. M. G. Harasewych & M. McNeilus, *Curasub*14-19, 25 September 2014; paratypes 22–25, RMNH.MOL.336199, off Substation Curaçao dock, Curaçao, 12°05.069′N, 68°53.886′W, 215–245 m, coll. A. Schrier, 31 March 2014.

Etymology: translucent (Latin), allowing light, but not detailed images, to pass through.

ZooBank registration: urn:lsid:zoobank.org:act:66BB0B6A-B02C-4A8B-B54D-829F38C673D7.

Diagnosis: Characteristics of genus, but shell large, thin, translucent.

Shell (Figs 1A–G, 2A–F): moderately large (to 41 mm), ovate, longer than high (shell length/height ratio SL/SH 1.2), equivalve, inequilateral, acline, somewhat inflated, with principle dissoconch growth gradient anterocrescent, with region of maximum convexity at approximately one third valve height from hinge margin. Shell strongly corrugated comarginally, extremely thin (56–96 μm), translucent, sinusoidal in radial section (amplitude to about 400 μm), with very fine, comarginal growth lines but without radial sculpture (Fig. 2C). Exterior sculpture concordant between valves. Hinge margin (Fig. 2D) short, straight, with orthogyrate umbones placed slightly anteriorly. Anterior margin straight, ventral and posterior margins broadly rounded. Shell colour whitish when dry, translucent to nearly transparent when wet. Dimensions ($n = 10$): height 24.9–34.2 mm, mean 29.8 ± 2.6 mm SD; length 30.3–40.6 mm, mean 35.5 ± 2.7 mm SD; hinge length 9.8–13.7 mm, 11.8 ± 1.1 mm SD.

Auricles, byssal notch and gapes: shell biauriculate, with larger posterior and smaller anterior auricles extremely weakly sinuated, coincident with adjacent shell margins. Commissural line straight. Byssal gape symmetrical, oriented anterodorsally, formed along slightly concave anterior shell margin. Wide posterior gape proximal to posterior extremity of hinge along dorsal part of posterior shell margin.

Muscle scars: interior shell surface smooth (Fig. 2D), with infrequent blister pearls (Fig. 2F). Posterior adductor muscle scar (Fig. 2D, pams) subcircular, situated posterodorsally, proximal to, but not adjacent to posterior shell margin. Two anterior ctenidial retractor muscles scars (Fig. 2D, acrms) subcircular, separate or confluent, situated anterodorsally to posterior adductor muscle scar. Anterior pedobyssal retracor muscle scars subcircular, situated on inner surface of anterodorsal shell margin ventral to anterior auricle. Three faint, subequal, irregularly shaped scars, corresponding to attachment areas of posterior pedobyssal retractor and two ctenidial retractor muscles situated ventral to posterior adductor muscle. Faint, small, irregularly shaped punctate pallial muscle scars densely distributed throughout anteroventral surface of valves. Two elongated, faint muscle scars placed ventral to hinge line anterior and posterior to resilifer. Pallial line continuous, frequently indistinct along anterior and posterior shell margins.

Hinge and ligament: hinge plate (Fig. 2D, hp) straight, moderately broad, edentulous. Ligamental (cardinal) area (Fig. 2D, E, lga) broadly triangular, symmetrical, occupying dorsal part of valves along entire length of hinge axis, extending to dorsal shell margin. Ligament alivincular, amphidetic, dorsal, submarginal. Ligamental layers continuous across valves with fibrous component (resilium) deposited in shallow, symmetrical, triangular resilifer (Fig. 2B, E, re) and lamellar component occupying flat ligamental area anterior and posterior to resilifer (Fig. 2B, re).

Larval shell: prodissoconch (Fig. 2A, B, pro) large (length 340 μm), hemispherical, cap-like, lacking prominent umbo, with straight hinge margin and rounded outline. Ontogenetically earliest shell (P1) could not be distinguished from veliger shell (P2). P2 sharply demarcated from early dissoconch by metamorphic line (Fig. 2A, mel).

Shell microstructure: shell (Fig. 2G, H) very thin (68 μm), composed of three distinct layers near ventral margin. Outermost layer (Fig. 2G, H, ol) (17 μm) composed of fine, presumably calcitic fibres. Middle layer (Fig. 2G, H, ml) is thickest (44 μm), consisting of crossed-lamellar, presumably aragonitic crystals. Innermost layer (Fig. 2G, H, il) (7 μm) composed of multiple layers of fine, possibly calcitic prisms.

Anatomy: Visceral mass (Fig. 3, vm): laterally compressed, small relative to size of shell, situated in anterodorsal region of shell ventral to hinge; posteroventral surface of visceral mass fused with anterior surface of posterior adductor muscle (Fig. 3, pam). Anteroventral extremity of visceral mass forms narrow ridge, extending medially from anterior surface of posterior adductor

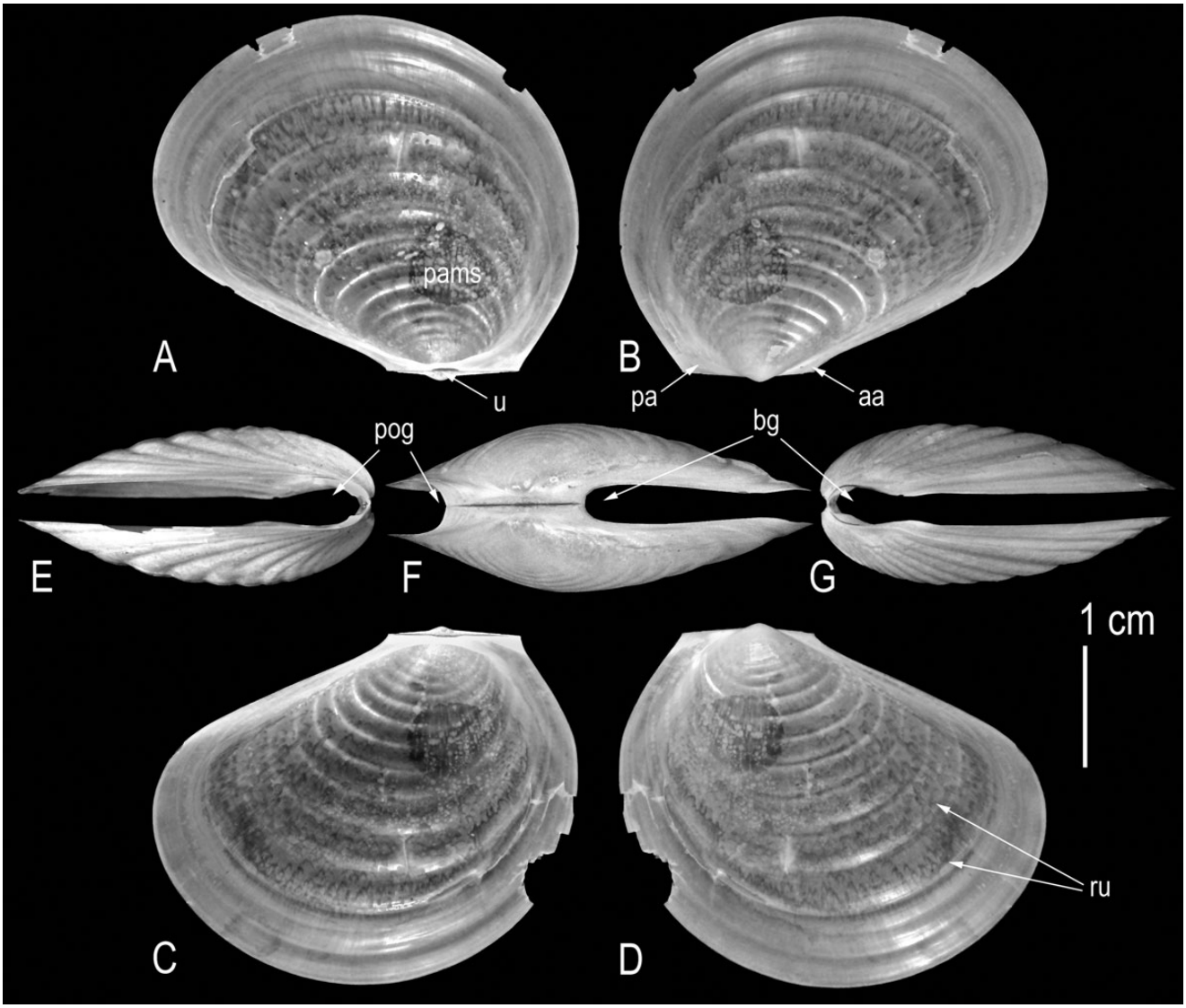

Figure 1. *Mantellina translucens* n. sp. Holotype (USNM1265094), off Sea Aquarium, Bapor Kibra, Willemstad, Curaçao. **A, B.** Inner and outer views of left valve. **C, D.** Inner and outer views of right valve. **E–G.** Posterior, dorsal and anterior views. Abbreviations: aa, anterior auricle; bg, byssal gape; pa, posterior auricle; pams, posterior adductor muscle scar; pog, posterior gape; ru, rugae; u, umbo.

muscle to foot on anterior surface of visceral mass. Visceral mass colourless and translucent in preserved specimens, yellowish orange in living specimens (Fig. 4A, C).

Musculature: adults monomyarian, with single large, cylindrical, posterior adductor muscle (Fig. 3, pam) situated posterodorsally, proximal to, but not adjacent to posterior shell margin. Posterior adductor muscle homogeneous, comprised exclusively of opaque, transverse 'catch' (slow) smooth fibres. Symmetrical anterior pedobyssal retractor muscles (Fig. 3, arm) extend dorsally from sides of base of foot (Fig. 3, f) to attachment points in subumbonal cavities in each valve; symmetrical posterior pedobyssal retractor muscles (Fig. 3, prm) extend ventrally and slightly posteriorly from dorsal side of base of foot to attachment points in midposterior surface in each valve ventral to posterior adductor muscle, passing in their course between posterior ctenidial retractor muscles and through ctenidial suspensory membrane (Fig. 3, sm). Ctenidia attached to shell by paired anterior (Fig. 3, acrm) and posterior (Fig. 3, pcrm) ctenidial retractor muscles. Anterior ctenidial retractor muscles pass through axes of descending lamellae of inner and outer demibranchs in each ctenidium and attach to shell proximal to labial palps, with attachment of inner demibranch retractor situated slightly dorsal to that of outer demibranch retractor. Posterior ctenidial retractor muscles pass through suspensory membrane, diverge at acute angle and form attachments on either side of attachment areas of posterior pedobyssal retractor muscles (Fig. 3, prm). Several bundles of radial pallial retractor muscles (Fig. 3, rprm) stretch from ventral and posteroventral margins of mantle to attachment areas on shell interior surfaces proximal to posterior pedobyssal retractor-posterior ctenidial retractor muscle attachment cluster (Fig. 3, prm + pcrm). Pallial muscle attachment areas formed by proximally fused pallial retractor muscle bundles.

Mantle: mantle lobes (Fig. 3, ml) extend from hinge axis around circumference of shell margin. Margins of left and right mantle lobes fused dorsally forming medial mantle isthmus (Fig. 3, mi). Area of dorsal fusion of inner folds of left and right mantle margins extends anteriorly beyond mantle isthmus, forming pallial hood concealing lips (Fig. 3, li), mouth and dorsal part of labial palps. Remaining mantle margins free. Inner surfaces of mantle lobes fused to lateral surfaces of visceral mass and to ventral edges of labial palps; exterior surfaces of mantle lobes attached to inner surfaces of valves by numerous, small, punctate attachment areas

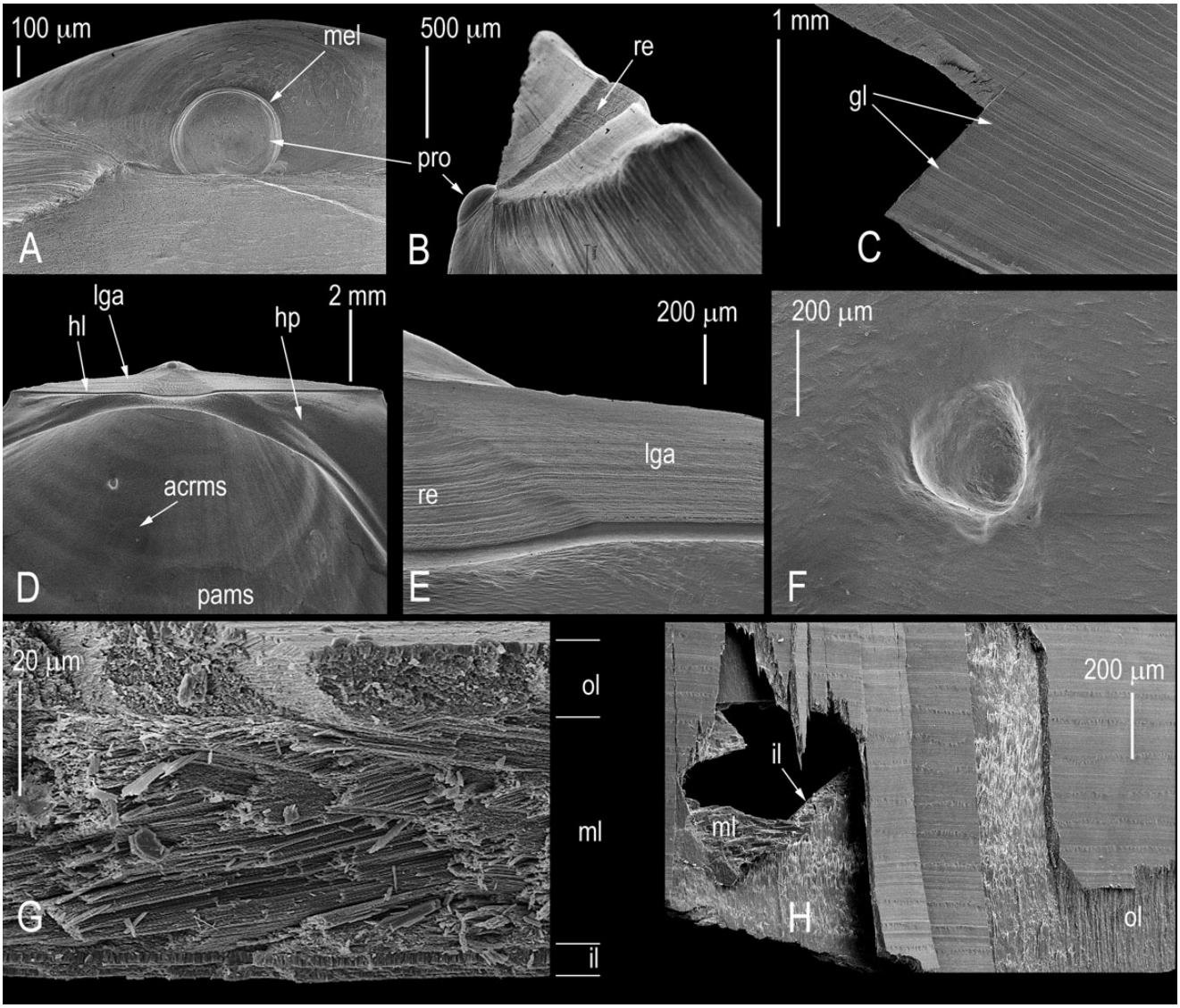

Figure 2. SEMs of shell of *Mantellina translucens* n. sp. **A–D.** Paratype 1 (USNM 1265095). **A, B.** Dorsal and anterior views of left umbone. **C.** Surface sculpture at posterior margin of right valve. **D.** Hinge area of right valve. **E.** Detail of ligamental plate. **F.** Detail of blister pearl in **D. G, H.** Paratype 2 (USNM 1265096). **G.** Cross section of shell parallel to growing edge near ventral shell margin. **H.** View of shell layers of broken shell fragment near growing edge. Abbreviations: acrms, anterior ctenidial retractor muscle scar; gl, growth lines; hl, hinge line; hp, hinge plate; il, inner shell layer; lga, ligamental area; mel, metamorphic line; ml, middle shell layer; ol, outer shell layer; pams, posterior adductor muscle scar, pro, prodissoconch; re, resilifer.

covering much of mantle lobe area. Mantle perforated by posterior adductor, pedobyssal and ctenidial retractor muscles. Supramyal septum (Fig. 3, ss) connecting inner surfaces of mantle lobes, stretching from posterodorsal surface of posterior adductor muscle to posterior extremity of mantle isthmus. Lateral surfaces of pericardial cavity formed by areas of mantle lobes connecting mantle isthmus to posterior adductor muscle, its posterior surface formed by supramyal septum, its anterior surface by the posterior surface of the visceral mass. Mantle thin, translucent, orange-red with areas of muscle attachments and punctate attachments of mantle lobes more strongly pigmented in living specimens (Fig. 4F, ppm). Marginal zone of mantle (mantle edge) subdivided into three folds. Outer and middle folds form inconspicuous, low ridges of approximately equal height; inner fold opaque, substantially exceeding other mantle folds in height and thickness, forming pallial veil (velum) (Fig. 4B). Inner and outer surfaces of all mantle folds smooth. Row of long, digitiform, conical, non-branched, distally tapering tentacles extend from base of inner fold (facing middle fold), spanning the circumference of the mantle along shallow grove between inner and middle folds. Most inner fold tentacles annulated, longitudinally grooved, but some are shorter (somewhat bottle-shaped), lack annulations, but with longitudinal groves. Long tentacles of inner fold alternate with one to three small, similarly shaped, annulated tentacles of varying size extending from base of middle fold proximal to grove between inner and middle folds. On average, tentacles longest at midposterior margin, more than twice the length of ventral margin tentacles; some unusually long tentacles occasionally found along anteroventral mantle margin. In living specimens middle fold tentacles orange, inner fold tentacles semitranslucent, the latter extremely long (may exceed three to four times shell length). Mantle margin considerably thicker than rest of mantle, with short radial muscles around entire periphery. Proximally, muscles attach to interior shell surface at base of mantle margin around periphery, forming a continuous pallial line; distally, muscles extend into bases of tentacles and diffuse into mantle margin. Mantle edge less translucent and more darkly pigmented than surfaces of mantle lobes.

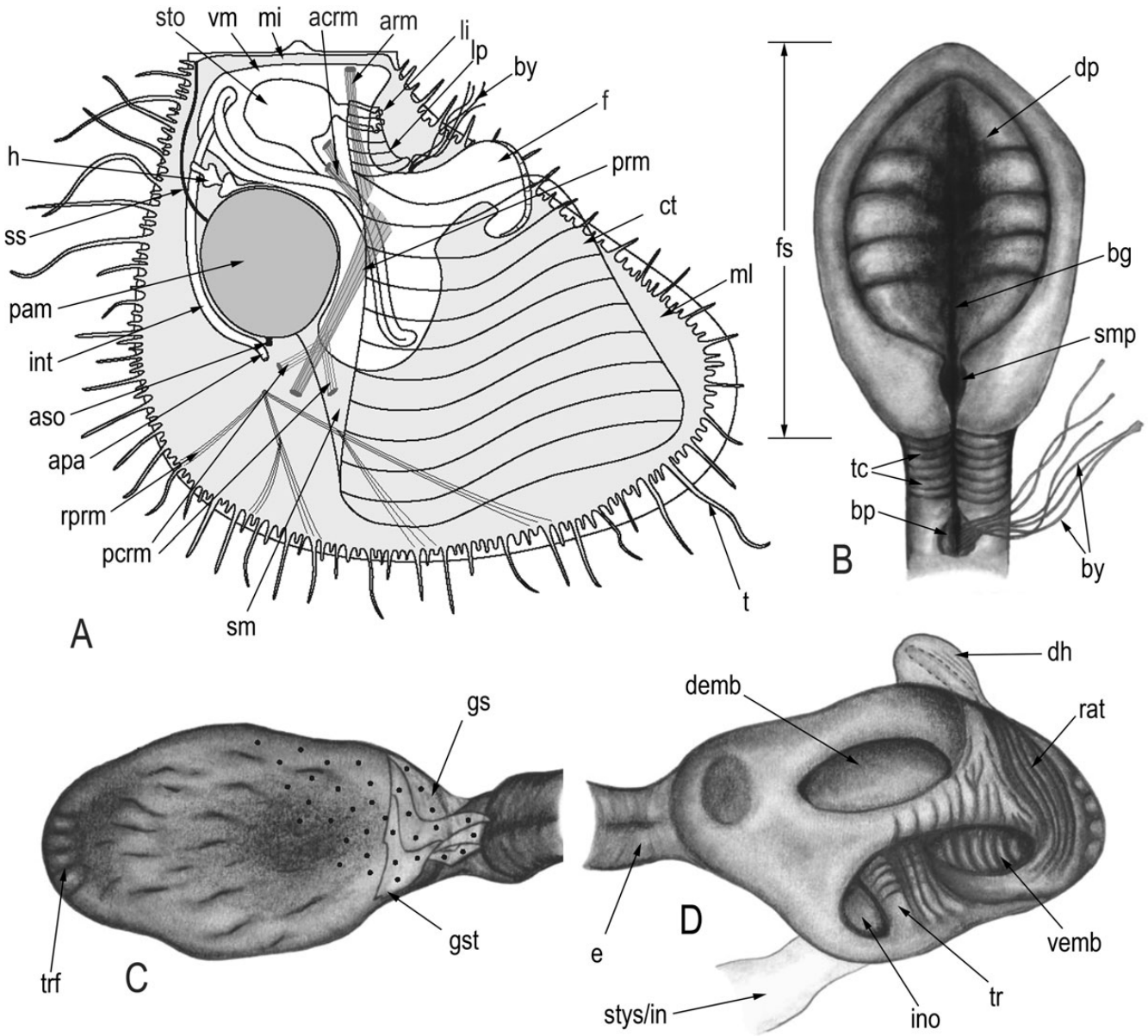

Figure 3. Gross anatomy of *Mantellina translucens* n. sp. **A.** Left lateral view of animal. **B.** Dorsal view of foot. **C, D.** Left anterodorsal and right wall of gastric chamber. Abbreviations: acrm, anterior ctenidial retractor muscles; apa, anal papilla; arm, anterior pedobyssal retractor muscles; aso, abdominal sense organs; bg, byssal groove; bp, byssal pit; by, byssus; ct, ctenidia; demb, dorsal embayment in stomach wall; dh, dorsal hood; dp, distal pit; e, oesophagus; f, foot; fs, tongue-shaped sole; gs, gastric shield; gst, gastric shield teeth; h, heart; ino, intestinal opening; int, intestine; li, lips; lp, labial palp; mi, mantle isthmus; ml, mantle lobes; pam, posterior adductor muscle; pcrm, posterior ctenidial retractor muscles; prm, posterior pedobyssal retractor muscles; rat, right wall acceptance tract; rprm, radial pallial retractor muscles; sm, ctenidial suspensory membrane; smp, small pit; ss, supramyal septum; sto, stomach; stys/in, merged style sac and midgut; t, pallial tentacle; tc, transverse corrugations; tr, transverse ridge; trf, transverse folds; vemb, ventral embayment in stomach wall; vm, visceral mass.

Foot and byssus: foot (Fig. 3A, f) large (relative to visceral mass), short, laterally compressed proximally, expanding distally into wide, dorsoventrally compressed, tongue-shaped sole (Fig. 3B, fs) with tapering, ventrally curling distal tip. Foot rotated 180° relative to its long axis, resulting in byssal groove (Fig. 3B, bg) oriented dorsally. Byssal groove extends medially from byssal pit (Fig. 3B, bp) at base of foot to large distal pit (Fig. 3B, dp) occupying nearly entire surface of sole. Small pit (Fig. 3B, smp) situated immediately proximal to distal pit. Surface of proximal part of foot with fine transverse corrugations (Fig. 3B, tc) bordering byssal groove. Byssus (Fig. 3A, B, by) emerges from laterally compressed opening of byssal groove at base of foot. Byssus of *c*. 30 nonmineralized, individual byssal threads. Byssal threads thin, translucent, light green, laterally compressed, flat (ribbon-like), with fine, regular, longitudinal striations, approximately uniform in width along length, slightly wider near distal extremity proximal to irregularly shaped, flat, adhesive plaques. Adhesive plaques of individual byssal threads often fused into common, irregularly shaped attachment surface. Proximal to their entry into visceral mass, byssal threads separate into symmetrical left and right bundles (without consolidating into byssal stems), forming V-shaped byssal root embedded in anterior region of visceral mass proximal to emergence of foot. Proximal extremities of byssal threads fuse laterally, producing

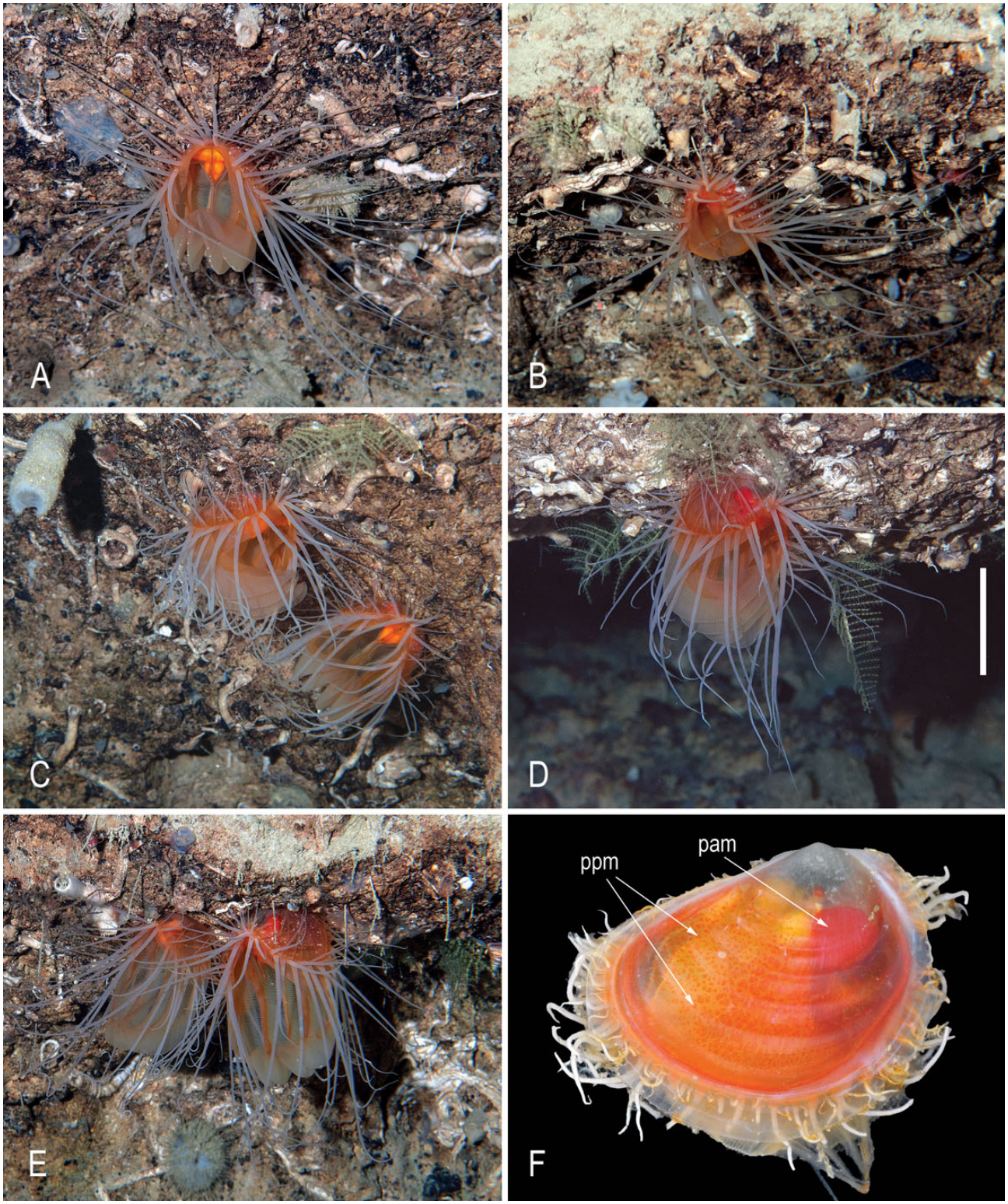

Figure 4. *In situ* photographs of living *Mantellina translucens* n. sp., occurring singly (**D**) or in pairs (**A + B, C, E**), attached by byssal threads to vertical wall of a rocky ridge off the Sea Aquarium, Bapor Kibra, Willemstad, Curaçao, at depths of 266–302 m. **A, B.** In 302 m, specimens about 40 cm apart. **C.** In 274 m. **D.** In 290 m. **E.** In 266 m. **F.** Left lateral view of specimen collected in 302 m. Photos courtesy of Substation Curaçao. Scale bar **A–F** = 5 cm. Abbreviations: pam, posterior adductor muscle; ppm, punctate pallial muscles.

irregularly shaped lamellose rootlets. Byssal rootlet lamellae form stacks, penetrate byssal gland, coming into close contact with left and right bundles of pedobyssal retractor muscles.

Labial palps: paired, symmetrical, projecting from their connection to lips ventrally towards base of foot along left and right anterolateral surfaces of visceral mass. Outer and inner folds

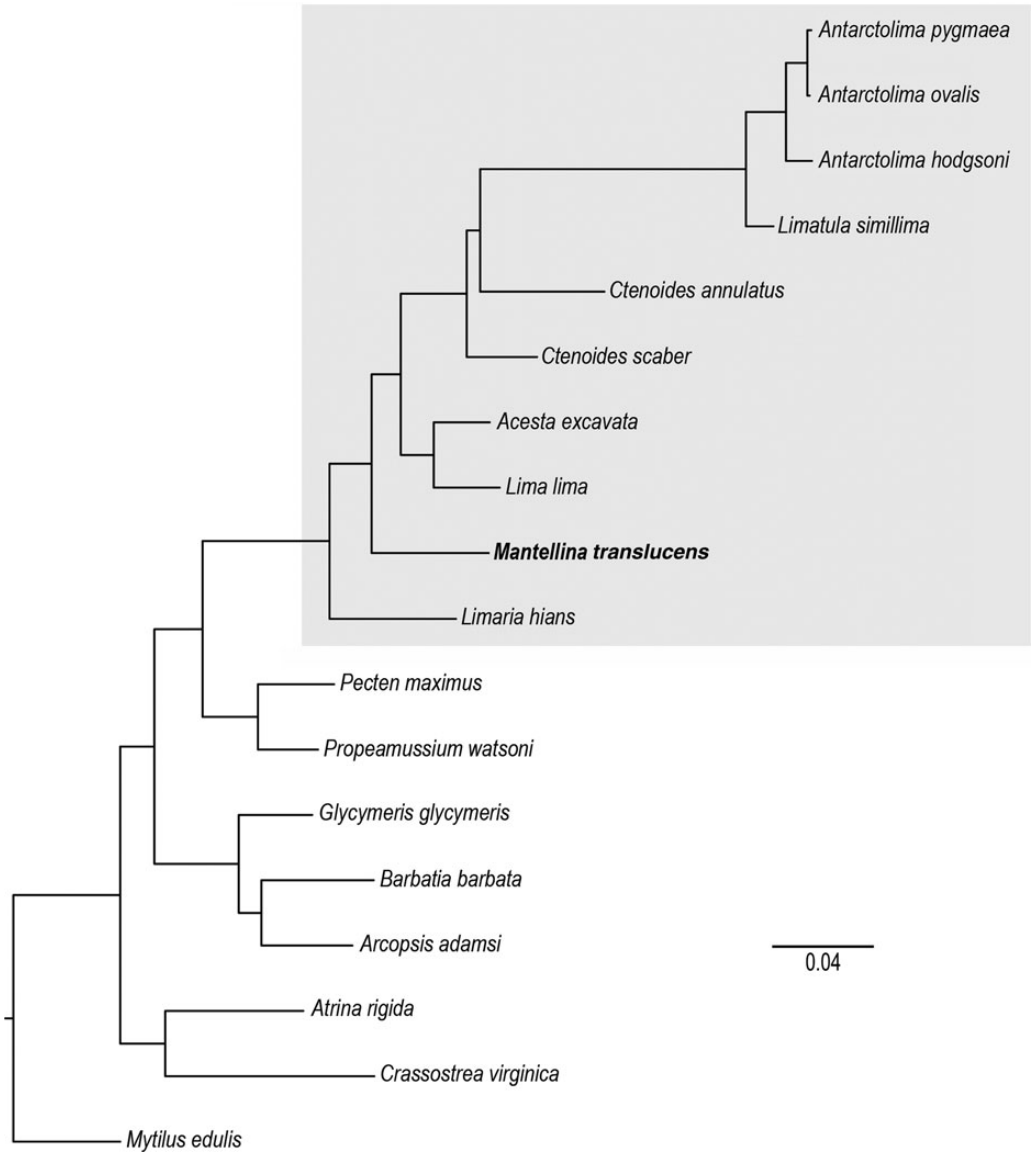

Figure 5. Phylogenetic relationships within Limidae (shaded box) based on maximum likelihood analysis (−logLk = 13304.06) of combined sequences from18S and 16S rDNA genes. The scale bar indicates the inferred number of substitutions per site. The topology of the tree is identical to parsimony analyses of the same dataset (see text for details). Jackknife support values were 100 % for all nodes (not shown).

continuous with upper and lower lips respectively. Each palp consists of outer and inner subrectangular folds attached to visceral mass along longer side, with anteriorly curving ventral extremity. Inner (opposing) surfaces of labial palps with 13–15 ciliated, parallel, transverse ridges; exterior surfaces smooth. Aboral side of palp ridges with secondary parallel ledge. Anterior filament of the inner demibranch not inserted into or fused with distal oral groove (labial palp-ctenidia association of Category III; Stasek, 1963).

Ctenidia (Fig. 3A, ct): large, symmetrical, translucent, plicate, broad, crescent-shaped (subquadrate in preserved specimens), occupying nearly entire mantle chamber, extending anteroventrally from posterior adductor muscle, roughly following outline of anteroventral shell margin. Ctenidia consist of inner and outer demibranchs with marginal food grooves. Inner demibranchs slightly longer than outer demibranchs. Dorsal edges of descending lamellae within demibranchs joined at ctenidial axes. Ctenidial axes fused to visceral mass proximally and attached to ventral surface of posterior adductor muscle distally by muscular suspensory membrane. Suspensory membrane diminished in height posteriorly. Dorsal margins of ascending lamellae of outer demibranchs not connected to inner surfaces of mantle lobes; dorsal margins of ascending lamellae of inner demibranchs not united medially (left and right ctenidia separate). Ctenidia may be extended far beyond the mantle cavity in living specimens (Fig. 4A, C–E). Filamental organization filibranch (adjacent filaments connected by ciliated disks produced from spurs on abfrontal surfaces of filaments and distributed in rows), heterorhabdic (differentiated ordinary and principal filaments). Serial tissue fusion of gill filaments restricted to dorsal edges of lamellae and ctenidial margins at point of junction of ascending and descending lamellae within each demibranch.

Digestive system: mouth slit-like, dorsoventrally compressed, concealed by anteriorly extending lips (Fig. 3A, li). Lateral extremities of lips with arborescent, interdigitating, transverse low ridges ('lip tentacles'); inner surfaces of lips with transverse grooves. Mouth opens into dorsoventrally flattened oesophagus (Fig. 3D, e). Irregular longitudinal grooves and ridges, continuous with transverse grooves and ridges of lips, extend into lumen

of oesophagus. Oesophagus smooth, capacious, entering gastric chamber ('stomach') (Fig. 3A, st) anteriorly and demarcated from it by a conspicuous constriction. Gastric chamber (Fig. 3A, st): globular, capacious, with length slightly exceeding height, placed centrally in visceral mass, enveloped by digestive gland. Posterior wall of gastric chamber with few irregular transverse folds (Fig. 3C, trf). Cuticle lines left anterodorsal surface of gastric chamber, with massive, gastric shield (Fig. 3C, gs) extending from region of constriction at juncture of stomach and oesophagus onto left anterodorsal surface; forming one or two indistinct gastric shield teeth (Fig. 3A, gst). Two conspicuous, horizontally orientated, blind pockets occupy most of right wall surface: smaller, blind, dorsal embayment (Fig. 3D, demb) with smooth surface and larger ventral embayment (Fig. 3D, vemb) with regular folds, grooves and openings of ducts of digestive diverticula. Ridge separating embayments curves along posteroventral edge of dorsal pocket and extends dorsally along gentle curve into dorsal hood (Fig. 3D, dh). Dorsal hood forms shallow pouch on posterodorsal surface of gastric chamber slightly displaced to right. Slightly recessed, narrow area posterior to ridge extends from dorsal hood towards intestinal opening on posteroventral side of gastric chamber, with longitudinal grooves (topologically corresponding to right wall acceptance tract, Fig. 3D, rat). Left pouch was not identified. Intestinal opening (Fig. 3D, io) located on posteroventral side of gastric chamber, bordered anteriorly by thick, longitudinally grooved, transverse ridge (Fig. 3D, tr). Transverse fold extending from floor of gastric chamber into ventral pocket of right wall. No distinct typhlosoles present in gastric chamber. Style sac and midgut merge to form single tube (Fig. 3D, stys/in). Descending arm of intestine (Fig. 3A, in) extends anteroventrally from gastric chamber, turns right proximal to ventralmost extremity of visceral mass, ascending arm runs parallel to descending arm along right side towards ventral surface of gastric chamber, curving towards posterodorsal surface of gastric chamber, making short loop to left, then dorsal and posterior in horizontal plane; upon exiting visceral mass, intestine penetrates pericardium, passing medially between ventricles, perforates supramyal septum, extends medially along posterior surface of posterior adductor muscle towards ventralmost extremity of visceral mass, terminating in short, free-hanging anal papilla (Fig. 3A, apa) that lacks anal funnel.

Heart and kidneys: heart (Fig. 3A, h) enclosed within pericardium situated between posterior surface of visceral mass and posterodorsal surface of posterior adductor muscle. Heart consists of symmetrical, paired ventricles, joined by narrow bridge dorsal to intestine and two dark grey, symmetrical, ventral auricles, fused along their ventral extremities, connecting to ventral pericardium via membranous extensions. Kidneys paired, laterally compressed, symmetrical, inconspicuous, transparent sacs with small dark brown speckles, fused to posterolateral surfaces of visceral mass.

Sense organs: paired abdominal sense organs (Fig. 3A, aso) form narrow ridges (colourless in preserved specimens), symmetrically placed on posteroventral surface of posterior adductor muscle, stretching ventrally along gentle arc towards lateral edges of adductor muscle proximal to anal papilla. Neither ctenidial ocelli nor mantle margin eyes are present.

Distribution: Presently known only from off the southeastern coast of Curacao, at depths of 215–305 m, attached to vertical rock surfaces by byssus.

Remarks: Mantellina translucens can be easily distinguished from all living species of Limidae on the basis of its anteroventrally elongated shell (SL/SH >1) that is extremely thin, nearly transparent, has broadly undulating comarginal corrugations and lacks radial sculptural elements (Table 2). These features are similar to those of several Cretaceous inoceramid taxa [e.g. *Inoceramya concentrica* Ulrich, 1904 from Alaska and *Sergipia posidonomyaformis* (Maury, 1935) from Brazil], but *M. translucens* differs in having a single, shallow triangular ligament pit rather than the multiple ligamental pits characteristic of inoceramids. Anatomical features such as a foot that is rotated 180° relative to the visceral mass and morphologically complex lips clearly place *Mantellina* within Limidae. Partial sequences for the nuclear 18S rDNA and mitochondrial 16S rDNA genes place *Mantellina* within Limidae and distinguish it from other genera with high levels of support.

PHYLOGENETIC ANALYSIS

A parsimony analysis of the molecular dataset performed under equal-costs regime produced a single, well resolved and strongly supported (JK = 100 % for all nodes) optimal cladogram (length L = 2964, consistency index CI = 0.76, retention index RI = 0.81); the same single topology was obtained under the parameter set that maximizes homology of both sequence fragments and base correspondences (L = 5835, CI = 0.29, RI = 0.43). A ML analysis of the same dataset resulted in a single tree with identical topology (−logLk = 13304.06; Fig. 5). The estimated shape parameter α of gamma distribution was 1.11; the substitution relative rate parameters for the model were 1.00 (AC), 2.43 (AG), 1.46 (AT), 0.60 (CG), 2.43 (CT), 1.00 (GT; fixed).

Limidae were recovered as a monophyletic clade within Pteriomorphia. *Mantellina translucens* nested within the family Limidae, derived relative only to *Limaria* and as sister taxon to the clade composed of the remaining representatives of Limidae. The genus *Ctenoides* was not monophyletic. The relationships among the species of *Limatula* concur with the findings of Page & Linse (2002), placing *L. pygmaea* (Philippi, 1845) and the subgenus *Antarctolima* Habe, 1977 in the genus *Limatula* S.V. Wood, 1839 rather than in *Limea* Bronn, 1831, as more recently advocated by Huber (2014).

DISCUSSION

Of the 10 living genera of Limidae, more than half have a fossil record extending into the Mesozoic, yet only *Mantellina* and *Limea* are based on fossil type species, both from Miocene deposits in the Paratethys Sea (Table 2). The type species of *Mantellina* was described from Miocene deposits of the Turin Hill area. Many of these deposits consist of mixed assemblages, where shallow water elements are associated with bathyal faunas (M. Taviani, personal communication), so the palaeoecology of *Mantellina* at this locality is uncertain. However, *M. labani* (Meznerics, 1936) from slightly older (Karpatian and Badenian) deposits of Slovakia, occurred in bathyal depths (200–300 m) (Harzhauser, Mandic & Schlögl, 2011), comparable to the depths that this genus inhabits in the Recent fauna, indicating that *Mantellina* has been a member of bathyal communities for at least 16 myr.

Relict pockets, regions with endemic faunas that have close affinities with faunas of earlier geological ages, have been reported from several areas along the southern Caribbean including the coasts of Colombia and Venezuela (Petuch, 1981, 2013). Most include relict species or genera represented in fossil deposits from the same geographic area. Like *Mantellina*, the genus *Lindapterys* Petuch, 1987 is known from Miocene deposits of the Paratethys, as well as from species living at bathyal depths in the southern Caribbean.

The conspicuous conchological similarities of *Mantellina* to several Cretaceous inoceramids was first noted by Sacco (1904), who named the type species *M. inoceramoides*. Although anatomical and molecular data clearly place *Mantellina* within Limidae, the apparent convergence in shell morphology is nevertheless quite striking (see Hammer, 2000).

Table 2. Features of Recent genera within Limidae and two genera of Inoceramidae.

TAXA	SL/SH	Equivalve	Radial sculpture	Comarginal ribs	Oldest record	Age of type species
Limidae						
Acesta	0.81	+	+	−	U Jurassic	Recent
Ctenoides	0.75	+	+	−	U Jurassic	Recent
Divarilima	0.93	+	+	−	Recent	Recent
Escalima	0.76	+	+	−	Recent	Recent
Lima	0.85	+	+	−	Jurassic	Recent
Limaria	0.91	+	+	−	Eocene	Recent
Limatula	0.67	+	+	−	Triassic	Recent
Antarctolima	0.79	+	+	−	Recent	Recent
Limea	0.85	+	+	−	Triassic	Miocene
Mantellina	1.19	+	−	+	Miocene	Miocene
Inoceramidae						
Inoceramya	1.14	+	−	+	Upper Cretaceous	Upper Cretaceous
Sergipia	1.23	+	−	+	Upper Cretaceous	Upper Cretaceous

Abbreviations: SL, shell length; SH, shell height.

Anatomical features of *M. translucens* largely conform to those previously reported for Limidae species, including the diagnostic features of the family: torsion of the foot by 180° relative to the visceral mass (Lacaze-Duthiers, 1854a; Seydel, 1909; Odhner, 1914; Lebour, 1937; Yonge, 1953; Gilmour, 1990), attachment of posterior pedobyssal retractor muscles posterior to the adductor muscle (Pelseneer, 1911) and bright orange-red colour of the mantle (Waller, 1976; Mikkelsen & Bieler, 2003, 2008).

The overall arrangement of muscles in *M. translucens* is similar to that of other limids, but the number and relative sizes of the pedobyssal retractor muscles as well as the relative placement of attachment areas of the posterior ctenidial and posterior pedobyssal retractor muscles vary among genera. *Mantellina translucens* most closely resembles species of *Limaria* (Seydel, 1909: Fig. E; Gilmour, 1990: Fig. 1F, G) in having single anterior and posterior pedobyssal retractors with small attachment areas on either side of the visceral mass. *Acesta excavata* and *Ctenoides scaber* have paired anterior and posterior pedobyssal retractors on both sides of the visceral mass, while in *Lima lima* there is one anterior and two posterior pedobyssal retractors; in these three species the pedobyssal retractors are strongly developed, with posterior retractors being particularly massive (Gilmour, 1990: Fig. 2).

Gilmour (1990) argued that pedobyssal muscles are differentiated into separate pedal and byssal muscles in byssate species of limids. Observations on *M. translucens* do not support this conclusion: despite the fact that adults of this species are byssate, they have single anterior and posterior pedobyssal retractors on each side of the visceral mass, as in abyssate adults of *Limaria*. A comparable degree of variation in the number and arrangement of pedobyssal retractors has been previously documented in Pterioidea (Tëmkin, 2006a: Fig. 18).

Despite similarities in pedobyssal musculature, foot morphology differs between *Mantellina* and *Limaria*: the sole of the foot of *L. tuberculata* is considerably smaller than that of *M. translucens*; the distal pit in *L. tuberculata* is smaller than the proximal pit (Seydel, 1909: pl. 31, Fig. 8; as '*Lima inflata*'), whereas in *M. translucens* the proximal pit is tiny relative to the massive distal pit (Seydel, 1909: pl. 31, Fig. 8; as '*Lima inflata*'). Such differences may be due to differences in the function of the foot and associated differences in the secretory epithelium: in *M. translucens*, the foot is concerned with planting the byssus, ensuring long term stabilization, whereas in species of *Limaria* it is used for locomotion and secretion of byssal threads for temporary attachment and nest construction (Barrois, 1885; Gilchrist, 1896; Seydel, 1909; Merrill & Turner, 1963; Gilmour, 1990).

Mantellina translucens lacks the hypertrophied anterior, posterior and accessory mantle retractor muscles, reported in *L. orientalis*, which are required for contractions used in swimming movements (Gilmour, 1990: Fig. 1F; as '*Limaria parafragile*'). Also, the posterior adductor muscle in *M. translucens* is homogenous, unlike the adductor in species of *Lima*, *Limaria* and *Acesta*, in which it is differentiated into a larger, striated anterior and narrow, crescent-shaped, unstriated posterior parts (Gilmour, 1990). Striated, or 'quick,' muscle fibres are responsible for the sudden contractions required for swimming and cleansing the mantle cavity, whereas the smooth unstriated, or 'catch' ('slow'), muscles provide prolonged adduction. This situation has a parallel in another pteriomorphian group, Pterioidea, where the only deep water species, *Pulvinites exempla*, has a homogeneous 'catch' adductor muscle (Tëmkin, 2006b).

Although *M. translucens* appears to lack muscular adaptations associated with swimming, it has been observed to swim briefly in captivity. Its limited capacity for swimming is consistent with the observation that the mantle margins are free in *M. translucens*, whereas in representatives of swimming species mantle margins are fused over nearly the entire length of the ventral margin (Stuardo, 1968). Posterior ctenidial muscles in *M. translucens* facilitate extension of the ctenidia between widely gaping valves, allowing for efficient filtration of large amount of water driven along radially arranged gill filaments. The protrusion of gills beyond the mantle cavity has been previously noted for other limids (Gilmour, 1990; Morton, 1979). Such an arrangement of ctenidia is presumed to produce a pattern of particle sorting similar to that found in lophophorates (Gilmour, 1978).

Pallial tentacles in Limidae display considerable variation in colour and morphology, and have been reported to be phylogenetically informative (reviewed by Mikkelsen & Bieler, 2003). The presence of annulations, papillae and tentacle length were considered to be generally consistent at the genus level. Unlike other limids, *M. translucens* possesses two distinct alternating types of tentacles: long semitranslucent tentacles of the inner fold and short orange tentacles of the middle folds; both types of tentacles are annulated. Differences in tentacle length were previously noted in *L. hians*, where more centrally placed and more glandular long tentacles were primarily secretory, participating in nest building, while shorter and more laterally placed tentacles were primarily sensory (Gilchrist, 1896; as '*Lima hians*'). The role of tentacles in nest building was also confirmed for *L. pellucida* (Merrill & Turner, 1963; as '*Lima pellucida*'). The longitudinal grooves along some of the tentacles in *M. translucens* are

reminiscent of the condition documented in species of *Ctenoides* (Mikkelsen & Bieler, 2003).

Tenticulate lips have been previously described for other limids (Pelseneer, 1906; Gilmour, 1964, 1974, 1990; Bernard, 1972; Mikkelsen & Bieler, 2003). The arborescent, low transverse ridges on the inner lateral surfaces of lips in *M. translucens* are more similar to the elaborate surface structures found in *L. hians* than to the interdigitating lamellae in *Acesta* and *Ctenoides* (Gilmour, 1964, 1974), but the lips in *M. translucens* are not fused over the oral groove. Lips in representatives of *Limatula* and *Limea* are devoid of tentacles (Gilmour, 1974).

The morphology of the gastric chamber has been previously studied in species of *Lima* (Mikkelsen & Bieler, 2003; Bieler *et al*., 2014), *Limaria* (Graham, 1949; Purchon, 1957; Reid, 1965) and *Ctenoides* (Mikkelsen & Bieler, 2003; Bieler *et al*., 2014) and has been classified as stomach type IV in Purchon's system (Purchon, 1957; Mikkelsen & Bieler, 2003, 2008).

The gastric chamber of *M. translucens* differs from the common limid plan in several respects. First, it is oriented horizontally, rather than vertically, as in all previously reported species. Second, there is a general simplification of the stomach structures, particularly on the left wall of the gastric chamber: various infoldings (such as the left pouch and food-sorting caecum) and grooved areas (presumed sorting areas) of the left side are absent. Third, no distinct typhlosoles extend into stomach lumen. The oesophagus of *M. translucens* is also substantially wider than that in other limids. This suite of characters, although developed to a greater degree, is characteristic of carnivorous habit across the Bivalvia (Tëmkin & Strong, 2013). Despite the fact that the gastric chamber of *M. translucens* conforms to the general morphology typical of suspension-feeding bivalves, our data raise the possibility that this species is potentially omnivorous, with a principal filter-feeding diet partly supplemented by unspecialized microphagy.

Ecology and morphological adaptations

It has been hypothesized that the adoption of the orthothetic mode in Limidae, facilitated by the development of bilateral symmetry between valves and the rotation of the foot, allowed for the evolution of efficient modes of filter feeding and mantle cavity cleansing (Gilmour, 1990). It was accompanied by a reduction in the protective function of the shell, development of defensive tentacles capable of autotomy, and secretion of predator deterring mucus (Gilmour, 1963, 1967, 1990). The extensive protrusion of ctenidia beyond the mantle cavity, large annulated tentacles and an extremely thin, equiconvex shell with a symmetrical byssal gape in *M. translucens* support this view.

This peculiar mode of feeding was suggested to have permitted species of limids (e.g. representatives of *Acesta* and *Limatula*; Hertlein, 1952; Fleming, 1978) to penetrate to the deeper regions of the oceans (Gilmour, 1990). *Mantellina translucens*, which occurs exclusively in bathyal depths, is characterized by a suite of characters—many unique within Limidae—reflecting its specialized adaptations to an epibyssate life mode in deep-water habitats. The most conspicuous character is the extremely thin, fragile and translucent shell, which offers little physical protection against predators, yet shells of some specimens bear multiple, presumably predator-induced, fractures that were successfully repaired, suggesting the possibility of chemical defense mechanisms (see Pawlik, 1993). Lack of hypertrophied development of the posterior pedobyssal retractors possibly reflects a lesser degree of reliance on strong byssal attachment for physical stabilization in less turbulent deeper waters, as evidenced from the morphology of the byssus, comprised of relatively few and very thin threads.

A number of distinctive prodissoconch characters—the lack of a distinct boundary between P1 and P2, a straight hinge line and the absence of a prominent umbo—suggests a lecithotrophic–planktotrophic reproductive mode, frequently correlated with brooding behaviour (Malchus, 2004). Occurrence of individuals of *M. translucens* in pairs is consistent with dioeciousness or protandry, both of which have been reported in Limidae (Lacaze-Duthiers, 1854b; Lodeiros & Himmelman, 1999).

Modifications of many features of the gastric chamber, typical of suspension-feeding bivalves, suggest that the feeding strategy of *M. translucens* is facultative omnivory, possibly associated with nutritionally impoverished environments below the photic zone. Consistent with adaptations to the aphotic zone is the lack of pallial eyes in *M. translucens*, which are considerably developed in species of *Ctenoides* and *Lima* (Waller, 1976; Mikkelsen & Bieler, 2003; reviewed by Morton, 2001 and Mikkelsen & Bieler, 2008).

Phylogenetic remarks

The primary goal of the phylogenetic analysis was to discern the systematic placement of *Mantellina*, rather than to resolve phylogenetic relationships within Limidae. Nevertheless, the analysis includes the broadest sampling (six of nine Recent genera) of the family to date. The molecular results are entirely concordant with prior studies containing a more limited sampling (Bieler *et al*., 2014: two genera; Steiner & Hammer, 2000: three genera; Page & Linse, 2002: four genera). Previous morphological studies of Limidae (Yonge, 1953; Stuardo, 1968; Mikkelsen & Bieler, 2003) suggested a suprageneric subdivision of the family into two clades, *Ctenoides-Lima-Acesta-Divarilima* and *Limaria-Limatula-Limea*, although phylogenetic analyses were not conducted. Our results based on the molecular data do not support the presence of the two major lineages within Limidae, although they suggest a close affinity between *Lima* and *Acesta*. Contrary to the assessment of Stuardo (1968), who considered *Limatula* to exhibit a more 'primitive' suite of characters, in our analyses *Limatula* was recovered as the most derived group. Echoing the conclusion drawn by Mikkelsen & Bieler (2003), our results call for a worldwide, comprehensive phylogenetic analysis of Limidae based on morphological and molecular evidence.

ACKNOWLEDGEMENTS

Fieldwork was conducted by the senior author as part of the Smithsonian Institution's Deep Reef Observation Project (DROP) aboard the *Curasub*, based at the Curaçao Sea Aquarium. Support from this programme is gratefully acknowledged. Thanks to Adriaan Schrier and the staff and crew of the Substation Curaçao and the Sea Aquarium for their hospitality and support. Special thanks to Marilee McNeilus and Cristina Castillo for assistance with the collection and processing of the specimens, and to Barry Brown and Daryl Felder for live animal photography. The assistance of Dr Amanda Windsor in generating the DNA sequence data is gratefully acknowledged, as is the assistance of Yolanda Villacampa in producing the SEM images. Thanks also to Prof. Marco Taviani for information on the paleoecology of the formations of the Turin Hills. We are grateful to Adam J. Baldinger (Museum of Comparative Zoology, Harvard University, Boston, USA) for lending us a copy of Stuardo's unpublished doctoral dissertation. We appreciate the helpful comments on shell microstructure by Prof. Antonio G. Checa (Departamento de Estratigrafía y Paleontología, Universidad de Granada, Granada, Spain). This is Ocean Heritage Foundation/Curaçao Sea Aquarium/Substation Curaçao (OHF/CSA/SC) Contribution Number 15.

REFERENCES

BARROIS, T. 1885. *Les glandes du pied et les pores aquifères chez les lamellibranches*. L. Danel, Lille.

BERNARD, F.R. 1972. Occurrence and function of lip hypertrophy in the Anisomyaria (Mollusca, Bivalvia). *Canadian Journal of Zoology*, **50**: 53–57.

BIELER, R., MIKKELSEN, P.M., COLLINS, T.M., GLOVER, E.A., GONZÁLEZ, V.L., GRAF, D.L., HARPER, E.M., HEALY, J., KAWAUCHI, G.Y., SHARMA, P.P., STAUBACK, S., STRONG, E.E., TAYLOR, J.D., TËMKIN, I., ZARDUS, J.D., CLARK, S., GUZMÁN, A., McINTYRE, E., SHARP, P. & GIRIBET, G. 2014. Investigating the Bivalve Tree of Life—an exemplar-based approach combining molecular and novel morphological characters. *Invertebrate Systematics*, **28**: 32–115.

COAN, E.V. & VALENTICH-SCOTT, P. 2012. *Bivalve seashells of tropical West America. Marine bivalve mollusks from Baja California to northern Peru*. Santa Barbara Museum of Natural History, Santa Barbara.

COSSMANN, M. 1905. Review of: I molluschi dei terreni terziarii del Piedmonte e della Liguria, Parte 30. *Revue Critique de Paléozoologie*, **9**: 89–90.

COX, L.R. & HERTLEIN, L.G. 1969. Family Limidae. In: *Part N [Bivalvia], Mollusca 6, vol. 1* (L.R. Cox et al., eds), pp. 385–393. In: *Treatise on invertebrate paleontology* (R.C. Moore, ed.). Geological Society of America and University of Kansas, Lawrence.

DARRIBA, D., TABOADA, G.L., DOALLO, R. & POSADA, D. 2012. jModelTest 2: more models, new heuristics and parallel computing. *Nature Methods*, **9**: 7–72.

DE LAET, J. 2005. Parsimony and the problem of inapplicables in sequence data. In: *Parsimony, phylogeny, and genomics* (V.A. Albert, ed.), pp. 81–116. Oxford University Press, New York.

FLEMING, C.A. 1978. The bivalve mollusc genus *Limatula*: a list of described species and a review of living and fossil species in the southwest Pacific. *Journal of the Royal Society of New Zealand*, **8**: 17–91.

GILCHRIST, J.D.F. 1896. *Lima hians* and its mode of life. *Transactions of the Natural History Society of Glasgow*, **4**: 218–225.

GILMOUR, T.H.J. 1963. A note on the tentacles of *Lima hians* (Gmelin) (Bivalvia). *Journal of Molluscan Studies*, **35**: 81–85.

GILMOUR, T.H.J. 1964. The structure, ciliation, and function of the lip-apparatus of *Lima* and *Pecten* [Lamellibranchia]. *Journal of the Marine Biological Association of the United Kingdom*, **44**: 485–498.

GILMOUR, T.H.J. 1967. The defensive adaptations of *Lima hians* (Mollusca, Bivalvia). *Journal of the Marine Biological Association of the United Kingdom*, **47**: 209–221.

GILMOUR, T.H.J. 1974. The structure, ciliation, and function of the lips of some bivalve molluscs. *Canadian Journal of Zoology*, **52**: 335–343.

GILMOUR, T.H.J. 1978. Ciliation and function of the food-collecting and waste-rejecting organs of lophophorates. *Canadian Journal of Zoology*, **56**: 2142–2155.

GILMOUR, T.H.J. 1990. The adaptive significance of foot reversal in the Limoida. In: *The Bivalvia—Proceedings of a memorial symposium in honour of Sir Charles Maurice Yonge (1899–1986), Edinburgh, 1986* (B. Morton, ed.), pp. 249–263. Hong Kong University Press, Hong Kong.

GIRIBET, G. 2005. Generating implied alignments under direct optimization using POY. *Cladistics*, **21**: 396–402.

GOFAS, S. 2014. Limidae Rafinesque, 1815. Accessed through: World Register of Marine Species at http://www.marinespecies.org/aphia.php?p=taxdetails&id=1778 on 18 July 2014.

GRAHAM, A. 1949. The molluscan stomach. *Transactions of the Royal Society of Edinburgh*, **61**: 737–778.

GUINDON, S., DUFAYARD, J.-F., LEFORT, V., ANISIMOVA, M., HORDIJK, W. & GASCUEL, O. 2010. New algorithms and methods to estimate maximum-likelihood phylogenies: assessing the performance of PhyML 3.0. *Systematic Biology*, **59**: 307–321.

HAMMER, Ø. 2000. A theory for the formation of comarginal ribs in mollusc shells by regulative oscillation. *Journal of Molluscan Studies*, **66**: 383–391.

HARASEWYCH, M.G., ADAMKEWICZ, S.L., BLAKE, J.A., SAUDEK, D., SPRIGGS, T. & BULT, C.J. 1997. Phylogeny and relationships of pleurotomariid gastropods (Mollusca: Gastropoda): an assessment based on partial 18S rDNA and cytochrome *c* oxidase I sequences. *Molecular Marine Biology and Biotechnology*, **6**: 1–20.

HARZHAUSER, M., MANDIC, O. & SCHLÖGL, J. 2011. A late Burdigalian bathyal mollusc fauna from the Vienna Basin (Slovakia). *Geologica Carpathica*, **62**: 211–231.

HERTLEIN, L.G. 1952. Description of a new pelecypod of the genus *Lima* from deep water off central California. *Proceedings of the California Academy of Sciences*, **27**: 377–381.

HUBER, M. 2010. *Compendium of bivalves*. ConchBooks, Hackenheim.

HUBER, M. 2014. *Limea pygmaea* (Philippi, 1845). Accessed through: World Register of Marine Species at http://www.marinespecies.org/aphia.php?p=taxdetails&id=505622 on 29 November 2014.

KATOH, K. & STANDLEY, D.M. 2013. MAFFT multiple sequence alignment software version 7: improvements in performance and usability. *Molecular Biology and Evolution*, **30**: 772–780.

LACAZE-DUTHIERS, H. 1854a. Memoire sur l'organisation de l'anatomie (*Anomia ephippium*). *Annales des Sciences Naturelles. Zoologie, Ser. 4*, **2**: 5–35.

LACAZE-DUTHIERS, H. 1854b. Recherches sur les organes genitaux des acephales lamellibranches. *Annales des Sciences Naturelles. Zoologie, Ser. 4*, **2**: 154–248.

LEBOUR, M.V. 1937. Larval and post-larval *Lima* from Plymouth. *Journal of the Marine Biological Association of the United Kingdom*, **21**: 705–710.

LODEIROS, C.J. & HIMMELMAN, J.H. 1999. Reproductive cycle of the bivalve *Lima scabra* (Pterioida: Limidae) and its association with environmental conditions. *Revista de Biología Tropical*, **47**: 411–418.

MALCHUS, N. 2004. Constraints in the ligament ontogeny and evolution of pteriomorphian Bivalvia. *Palaeontology*, **47**: 1539–1574.

MEDLIN, L.K., ELWOOD, H.J., STICKEL, S. & SONGIN, M.L. 1988. The characterization of enzymatically amplified eukaryotic lds-like rRNA coding regions. *Gene*, **71**: 491–499.

MERRILL, A.S. & TURNER, R.D. 1963. Nest building in the bivalve genera *Musculus* and *Lima*. *Veliger*, **6**: 55–59.

MEZNERICS, I. 1936. Die Schlierbildungen des mittelsteirischen Beckens. *Mitteilungen des Naturwissenschaftlichen Vereines für Steiermark*, **73**: 118–140.

MIKKELSEN, P.M. & BIELER, R. 2003. Systematic revision of the western Atlantic file clams, *Lima* and *Ctenoides* (Bivalvia: Limoida: Limidae). *Invertebrate Systematics*, **17**: 667–710.

MIKKELSEN, P.M. & BIELER, R. 2008. *Seashells of southern Florida. Bivalves*. Princeton University Press, Princeton.

MORTON, B. 1979. A comparison of lip structure and function correlated with other aspects of the functional morphology of *Lima lima*, *Limaria* (*Platilimaria*) *fragilis*, and *Limaria* (*Platilimaria*) *hongkongensis* sp. nov. (Bivalvia: Limacea). *Canadian Journal of Zoology*, **57**: 728–742.

MORTON, B. 2001. The evolution of eyes in the Bivalvia. *Oceanography and Marine Biology: an Annual Review*, **39**: 165–205.

ODHNER, N.H. 1914. Notizen über die Fauna der Adria bei Rovigno. Beiträge zur Kenntnis der marinen Molluskenfauna von Rovigno in Istrien. *Zoologischer Anzeiger*, **44**: 156–170.

PAGE, T.J. & LINSE, K. 2002. More evidence of speciation and dispersal across the Antarctic Polar Front through molecular systematics of Southern Ocean *Limatula* (Bivalvia: Limidae). *Polar Biology*, **25**: 818–826.

PALUMBI, S. 1996. Nucleic acids II: the polymerase chain reaction. In: *Molecular systematics* (D. Hillis, C. Moritz & B.K. Mable, eds), pp. 205–247. Sinauer Associates, Sunderland, MA.

PAWLIK, J.R. 1993. Marine invertebrate chemical defenses. *Chemical Review*, **93**: 1911–1922.

PELSENEER, P. 1906. Un genre de lamellibranches à bouches multiples. *Comptes Rendus Hebdomadaires des Séances de l'Académie des Sciences*, **142**: 722–723.

PELSENEER, P. 1911. Les lamellibranches de l'expédition du Siboga. Partie Anatomique. *Siboga-Expeditie*, **53a**: 1–125.

PETUCH, E.J. 1981. A relict caenogastropod fauna from northern South America. *Malacologia*, **20**: 307–334.

PETUCH, E.J. 2013. *Biogeography and biodiversity of western Atlantic mollusks*. CRC Press, Boca Raton.

PURCHON, R.D. 1957. The stomach in the Filibranchia and Pseudolamellibranchia. *Proceedings of the Zoological Society of London*, **129**: 27–60.

REID, R.G.B. 1965. The structure and function of the stomach in bivalve molluscs. *Journal of Zoology*, **147**: 156–184.

ROSENBERG, G. 2009. Malacolog 4.1.1: A database of Western Atlantic marine Mollusca. [WWW database (version 4.1.1)] URL http://www.malacolog.org/.

SACCO, F. 1904. *I molluschi dei terreni terziarii del Piedmonte e della Liguria, Parte 30: Aggiunte e Correzioni. Considerazioni generali. Indice generale dell'opera*. Clausen, Torino.

SCHULTZ, O. 2001. Bivalvia neogenica (Nuculacea-Unionacea). In: *Catalogus fossilium Austriae. Vol. 1, part 1* (W.E. Piller, ed.), pp. 1–379. Österreichischen Akademie der Wissenschaften, Wien.

SEYDEL, E. 1909. Untersuchungen über den Byssusapparat der Lamellibranchiaten. *Zoologische Jahrbücher, Abteilung für Anatomie und Ontogenie der Tiere*, **27**: 465–582.

STASEK, C.R. 1963. Synopsis and discussion of the association of ctenidia and labial palps in the bivalve Mollusca. *Veliger*, **6**: 91–97.

STEINER, G. & HAMMER, S. 2000. Molecular phylogeny of the Bivalvia inferred from 18S rDNA sequences with particular reference to the Pteriomorphia. In: *The evolutionary biology of the Bivalvia* (E.M. Harper, J.D. Taylor & J.A. Crame, eds), pp. 11–29. Geological Society of London.

STUARDO, J.R. 1968. *On the phylogeny, taxonomy and distribution of the Limidae (Mollusca: Bivalvia)*. PhD thesis, Harvard University.

TËMKIN, I. 2006a. Morphological perspective on classification and evolution of Recent Pterioidea (Mollusca: Bivalvia). *Zoological Journal of the Linnean Society*, **148**: 253–312.

TËMKIN, I. 2006b. Anatomy, shell morphology, and microstructure of the living fossil *Pulvinites exempla* (Hedley, 1914) (Bivalvia: Pulvinitidae). *Zoological Journal of the Linnean Society*, **148**: 523–552.

TËMKIN, I. & STRONG, E.E. 2013. New insights on stomach anatomy of carnivorous bivalves. *Journal of Molluscan Studies*, **79**: 332–339.

VARÓN, A., LUCARONI, N., HONG, L. & WHEELER, W.C. 2013. POY 5:0. American Museum of Natural History, New York. http://www.amnh.org/our-research/computational-sciences/research/projects/systematic-biology/poy.

VOKES, H.E. 1967. Genera of the Bivalvia: a systematic and bibliographic catalogue. *Bulletins of American Paleontology*, **51**: 103–394.

WALLER, T.R. 1976. The behavior and tentacle morphology of pteriomorphian bivalves: a motion-picture study. *Bulletin of the American Malacological Union*, **1975**: 7–13.

WHEELER, W.C. 1996. Optimization alignment: the end of multiple sequence alignment in phylogenetics? *Cladistics*, **12**: 1–9.

WHEELER, W.C. 2001. Homology and the optimization of DNA sequence data. *Cladistics*, **17**: S3–S11.

WHEELER, W.C. 2003a. Implied alignment: a synapomorphy-based multiple-sequence alignment method and its use in cladogram search. *Cladistics*, **19**: 261–268.

WHEELER, W.C. 2003b. Iterative pass optimization of sequence data. *Cladistics*, **19**: 254–260.

YONGE, C.M. 1953. The monomyarian condition in the Lamellibranchia. *Transactions of the Royal Society of Edinburgh*, **62**: 443–478.